Inorganic Chemistry

Article

pubs.acs.org/IC

A Ratiometric Luminescence Probe for Highly Reactive Oxygen Species Based on Lanthanide Complexes

Yunna Xiao, Zhiqiang Ye,* Guilan Wang, and Jingli Yuan*

State Key Laboratory of Fine Chemicals, School of Chemistry, Dalian University of Technology, Dalian 116024, People's Republic of China

Supporting Information

ABSTRACT: Reactive oxygen species (ROS) are important mediators in a variety of pathological events, but the oxidative stress owing to excessive generation of ROS is implicated in many human diseases. In this work, we designed and synthesized a novel dual-functional chelating ligand, [4′-(*p*-aminophenoxy)methylene-2,2′:6′,2″-terpyridine-6,6″-diyl]-bis(methylenenitrilo)tetrakis(acetic acid) (AMTTA), that can strongly coordinate with both Eu^{3+} and Tb^{3+} in aqueous solutions for the recognition and time-gated luminescence detection of highly ROS (hROS), hydroxyl radical ($^{\bullet}OH$), and hypochlorite (ClO^-). The complexes AMTTA-Ln^{3+} (Ln = Eu and Tb) are almost nonluminescent because of the photoinduced electron transfer from the electron-rich aminophenyl group to the terpyridine-Ln^{3+} moiety but can rapidly react with hROS to afford highly luminescent complexes (4′-hydroxymethyl-2,2′:6′,2″-terpyridine-6,6″-diyl)bis(methylenenitrilo)tetrakis(acetate)-Ln^{3+} (HTTA-Ln^{3+}). Interestingly, when the AMTTA-Eu^{3+}/Tb^{3+} mixture (AMTTA/Eu^{3+}/Tb^{3+} = 2/1/1) was reacted with hROS, the intensity ratio of its Tb^{3+} emission at 540 nm to its Eu^{3+} emission at 610 nm, I_{540}/I_{610}, showed a ratiometric response toward hROS, and the dose-dependent increase of the ratio displayed a double-exponential correlation to the concentration of hROS. This unique luminescence response allowed the AMTTA-Eu^{3+}/Tb^{3+} mixture to be used as a ratiometric probe for the time-gated luminescence detection of hROS.

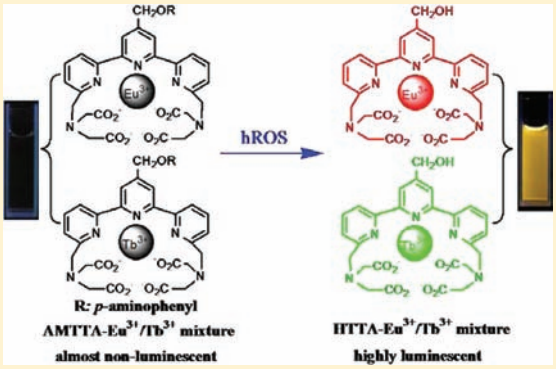

INTRODUCTION

Reactive oxygen species (ROS), including alkylperoxyl radicals ($ROO^{\bullet}$), superoxide anion radical ($O_2^{\bullet-}$), hydrogen peroxide (H_2O_2), singlet oxygen ($^1O_2$), hypochlorite (ClO^-), hydroxyl radical ($^{\bullet}OH$), and so on, are collective terms representing the chemical species that are formed from the incomplete reduction of oxygen.[1−3] It has been known that ROS are important signaling molecules in biological systems to regulate a wide range of physiological functions, but their overproduction can result in oxidative stresses, which are involved in the pathogenesis of many diseases, such as carcinogenesis,[4] inflammation,[5] ischemia-reperfusion injury,[6] cardiovascular disease, and neurological disorders.[7−10] Therefore, detection methods for ROS could be powerful tools to elucidate the molecular mechanisms that underlie such physiological and pathological conditions.[11] In various methods, fluorescence analysis in combination with a ROS-responsive luminescence probe is generally considered to be one of the most promising methods because of its high sensitivity, selectivity, experimental feasibility, and convenience in data collection.[12]

To date, a variety of fluorescent probes for the detection of ROS have been developed. The generally used probes, such as 2,7-dichlorodihydrofluorescein[13a] and dihydrorhodamine 123,[13b] can be oxidized by various ROS to afford strong luminescence signals, but they lack the recognition selectivity to distinguish a specific ROS. To solve this problem, many efforts have been motivated to develop fluorescent probes that can distinguish an individual species of ROS in recent years.[14] Among various ROS, ClO^- and $^{\bullet}OH$ are considered to be highly ROS (hROS) because of their strong oxidant property that can directly oxidize DNA-duplex, proteins, and lipids.[15] Thus, the development of fluorescent probes for detecting hROS in vivo and in vitro remains an active and challenging work. To this end, several organic dye-based fluorescence probes that can selectively respond to hROS, such as 2-[6-(4′-hydroxy)phenoxy-3*H*-xanthen-3-on-9-yl]benzoic acid and 2-[6-(4′-amino)phenoxy-3*H*-xanthen-3-on-9-yl]benzoic acid[15] and MitoAR and MitoHR,[16] have been developed and used for imaging hROS production in living cells.

In most cases, the responses of fluorescent probes to analytes are based on the increase or decrease of the fluorescence intensities of the probes, which have an unavoidable critical problem that the signal intensity could be influenced by many factors, e.g., excitation intensity, probe concentration, sample environment, etc. In contrast to the intensity-based probes, a ratiometric fluorescence probe can get rid of most or all of these impacts by the self-calibration of two emission bands at

Received: October 11, 2011
Published: February 22, 2012

   dx.doi.org/10.1021/ic202195a | *Inorg. Chem.* 2012, 51, 2940−2946

Scheme 1. Luminescence Response Reaction of the AMTTA-Eu^{3+}/Tb^{3+} Mixture toward hROS[a]

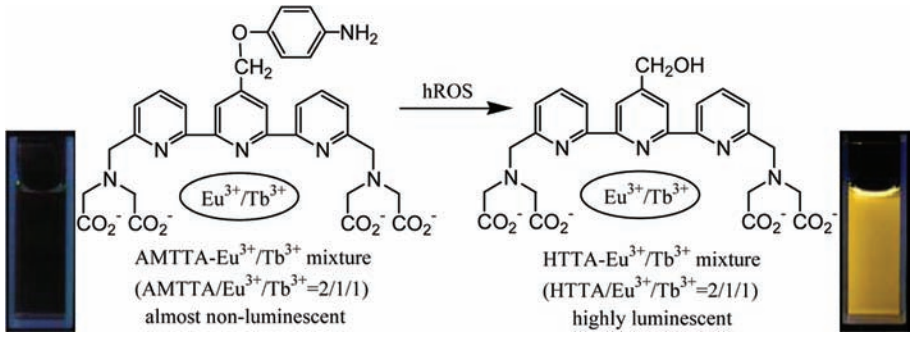

[a]The photographs show the luminescence colors of the complex solutions under a 365 nm UV lamp.

different wavelengths to increase the accuracy of the fluorescence measurement.[17] Furthermore, the fluorescence measurement for a complicated biological sample is also profoundly interfered by the strong autofluorescence from the sample. On the basis of the above opinions, we have attempted to develop ratiometric luminescence probes based on the luminescent lanthanide complexes because their sharp and long-lived emissions enable them to be ideal probes for time-gated luminescence detection to discriminate the background noises, and the dilanthanide ensemble consisting of a mixture of Eu^{3+}/Tb^{3+} complexes can be easily used to generate ratiometric luminescence probes.[18]

In this work, a novel dual-functional chelating ligand, [4′-(*p*-aminophenoxy)methylene-2,2′:6′,2″-terpyridine-6,6″-diyl]bis-(methylenenitrilo)tetrakis(acetic acid) (AMTTA), that can strongly coordinate with both Eu^{3+} and Tb^{3+} and specifically react with hROS in aqueous solutions was designed and synthesized. Its complexes with Ln^{3+} ions, AMTTA-Ln^{3+} (Ln = Eu and Tb), are highly stable and water-soluble and almost nonluminescent because of photoinduced electron transfer (PET) from the electron-rich *p*-aminophenyl group to the terpyridine-Ln^{3+} moiety. However, upon reaction with hROS, due to cleavage of the *p*-aminophenyl ether in the complex, the highly luminescent complexes (4′-hydroxymethyl-2,2′:6′,2″-terpyridine-6,6″-diyl)bis(methylenenitrilo)tetrakis(acetate)-Ln^{3+} (HTTA-Ln^{3+}) can be generated. It was found that the AMTTA-Eu^{3+}/Tb^{3+} mixture (AMTTA/Eu^{3+}/Tb^{3+} = 2/1/1) showed a ratiometric luminescence response to hROS. The intensity ratio of its Tb^{3+} emission at 540 nm to its Eu^{3+} emission at 610 nm, I_{540}/I_{610}, could be remarkably augmented upon reaction with hROS. Thus, a ratiometric and time-gated luminescence detection method for hROS using the AMTTA-Eu^{3+}/Tb^{3+} mixture as a probe was developed. Scheme 1 shows the structures of AMTTA-Eu^{3+}/Tb^{3+} and HTTA-Eu^{3+}/Tb^{3+} and the luminescence response reaction of AMTTA-Eu^{3+}/Tb^{3+} toward hROS.

EXPERIMENTAL SECTION

Materials and Physical Measurements. Ethyl 6,6″-bis-(bromomethyl)-2,2′:6′,2″-terpyridine-4′-carboxylate (compound **1**) was synthesized according to a previously reported method.[19] Tetrahydrofuran (THF) and acetonitrile were used after appropriate distillation and purification. 1-Hydroxy-2-oxo-3-(3-aminopropyl)-3-methyl-1-triazene (NOC-13, a NO donor with a half-life of 13.7 min) was synthesized using a reported method.[20] Hydrogen peroxide (H_2O_2) was diluted immediately from a stabilized 30% solution and was assayed by using its molar absorption coefficient of 43.6 cm^{-1} M^{-1} at 240 nm.[21] Hydroxyl radical ($^{\bullet}OH$) was generated in the Fenton system from ferrous ammonium sulfate and H_2O_2.[22] Peroxynitrite (NaONOO) was synthesized from sodium nitrite (0.6 M) and H_2O_2 (0.65 M) in a quenched-flow reactor (excess H_2O_2 was used to minimize nitrite contamination).[23] After the reaction, the solution was treated with MnO_2 to eliminate the excess H_2O_2. The concentration of the NaONOO stock solution was determined by measuring the absorbance at 302 nm with a molar extinction coefficient of 1670 cm^{-1} M^{-1}.[24] Singlet oxygen ($^1O_2$) was generated from the Na_2MoO_4/H_2O_2 system in 0.05 M carbonate buffer of pH 10.5.[25] Superoxide anion radical ($O_2^{\bullet-}$) was generated from the xanthine−xanthine oxidase system.[26] A stock solution of ClO^- was prepared from a commercial sodium hypochlorite solution. Unless otherwise specified, all chemical materials were purchased from commercial sources and used without further purification.

^1H and ^{13}C NMR spectra were recorded on a Bruker Avance spectrometer (400 MHz for ^1H and 100 MHz for ^{13}C). Electrospray ionization mass spectrometry (ESI-MS) spectra were measured on a HP1100LC/MSD electrospray ionization mass spectrometer. Elemental analysis was carried out on a Vario-EL CHN analyzer. Absorption spectra were measured on a Perkin-Elmer Lambda 35 UV−vis spectrometer. All time-gated luminescence spectra and luminescence properties were measured on a Perkin-Elmer LS 50B luminescence spectrometer with the following settings: delay time, 0.2 ms; gate time, 0.4 ms; cycle time, 20 ms; excitation slit, 10 nm; emission slit, 5 nm. The luminescence quantum yields of AMTTA-Ln^{3+} and HTTA-Ln^{3+} were measured by using the previous methods.[18c,27]

Syntheses of AMTTA and HTTA. The reaction pathways for the synthesis of AMTTA and HTTA are shown in Scheme S1 in the Supporting Information, and the details are described as follows.

4′-Hydroxymethyl-6,6″-bis(bromomethyl)-2,2′:6′,2″-terpyridine (2). $LiAlH_4$ (183.1 mg, 4.82 mmol) was added slowly into a solution of compound **1** (1.05 g, 2.21 mmol) in dry THF (80 mL) at 0 °C, and the suspension was stirred for 2.5 h in an ice−water bath. After the precipitate was removed by filtration and washed three times with dry THF, the filtrate was evaporated. The residue was purified by silica gel column chromatography with CH_2Cl_2/CH_3OH (100/1, v/v) as the eluent to afford compound **2** as a white solid (246 mg, 25% yield). ^1H NMR (400 MHz, $CDCl_3$): δ 4.66 (s, 4H), 4.97 (s, 2H), 7.51 (d, J = 8.0 Hz, 2H), 7.86 (t, J = 7.8 Hz, 2H), 8.49 (d, J = 7.8 Hz, 2H), 8.56 (s, 2H). ^{13}C NMR (100 MHz, $CDCl_3$): δ 34.02, 63.85, 118.95, 120.59, 123.74, 137.98, 153.72, 156.29, 156.82, 158.76. ESI-MS (m/z): 472.0 ($[M + Na]^+$, 100%), 450.0 ($[M + H]^+$, 20%).

Tetraethyl (4′-Hydroxymethyl-2,2′:6′,2″-terpyridine-6,6″-diyl)bis(methylenenitrilo)tetrakis(acetate) (3). Diethyl iminodiacetate (356.8 mg, 3.49 mmol) and NaH (110 mg, 4.58 mmol) were added into dry acetonitrile (20 mL) under an argon atmosphere. After the suspension was stirred for 1 h, a solution of compound **2** (680 mg, 1.52 mmol) in dry THF (15 mL) was poured into the above suspension. The mixture was further stirred overnight under an argon atmosphere. After the precipitate was removed by filtration and washed three times with dry THF, the filtrate was evaporated, and the residue was purified by silica gel column chromatography with

dx.doi.org/10.1021/ic202195a | *Inorg. Chem.* 2012, 51, 2940−2946

petroleum ether/ethyl acetate (1/1, v/v) as the eluent to afford compound **3** as yellowish crystals (560 mg, 56% yield). ^{1}H NMR (400 MHz, $CDCl_3$): δ 1.24 (t, J = 6.0 Hz,12H), 3.68 (s, 8H), 4.14−4.21 (m, 12H), 4.87 (s, 2H), 7.60 (d, J = 8.0 Hz, 2H), 7.82 (t, J = 7.8 Hz, 2H), 8.41 (s, 2H), 8.43 (d, J = 7.8 Hz, 2H). ^{13}C NMR (100 MHz, $CDCl_3$): δ 14.21, 55.09, 59.46, 60.72, 61.56, 119.47, 120.46, 123.87, 138.80, 153.52, 153.61, 157.84, 169.42, 171.15. ESI-MS (m/z): 666.3 ([M + H]$^+$, 100%), 688.3 ([M + Na]$^+$, 45%).

Tetraethyl (4′-Bromomethyl-2,2′:6′,2″-terpyridine-6,6″-diyl)bis(methylenenitrilo)tetrakis(acetate) (4). To a solution of compound **3** (550 mg, 0.83 mmol) in 15 mL of dry THF was added dropwise PBr_3 (268.2 mg, 1.00 mmol) with stirring. After the solution was stirred for 2 h at room temperature, 150 mL of $CHCl_3$ was added. The solution was washed three times with 100 mL of water and dried with Na_2SO_4. The solvent was evaporated, and then the residue was purified by silica gel column chromatography with petroleum ether/ethyl acetate (2/1, v/v) as the eluent to afford compound **4** as a white oil (390 mg, 65% yield). ^{1}H NMR (400 MHz, $CDCl_3$): δ 1.26 (t, J = 6.0 Hz, 12H), 3.71 (s, 8H), 4.17−4.22 (m, 12H), 4.59 (s, 2H), 7.66 (d, J = 8.0 Hz, 2H), 7.85 (t, J = 7.6 Hz, 2H), 8.49 (s, 2H), 8.51 (s, 2H). ^{13}C NMR (100 MHz, $CDCl_3$): δ 14.24, 55.03, 59.67, 60.73, 61.71, 119.89, 120.50, 123.69, 138.26, 155.47, 155.29, 157.79, 167.68, 171.00. ESI-MS (m/z): 728.3/730.3 ([M + H]$^+$, 100%), 750.3/752.3 ([M + Na]$^+$, 90%).

Tetraethyl [4′-(*p*-Aminophenoxy)methylene-2,2′:6′,2″-terpyridine-6,6″-diyl]bis(methylenenitrilo)tetrakis(acetate) (5). After a mixture of *p*-aminophenol (197.9 mg, 1.82 mmol) and NaH (44 mg, 1.82 mmol) in 20 mL of dry acetonitrile was stirred at room temperature for 15 min under an argon atmosphere, compound **4** (440 mg, 0.61 mmol) was added. The suspension was further stirred overnight under an argon atmosphere. After filtration, the solvent was evaporated, and the residue was purified by silica gel column chromatography with CH_2Cl_2/CH_3OH (40/1, v/v) as the eluent to afford compound **5** as a yellow oil (230 mg, 50% yield). ^{1}H NMR (400 MHz, $CDCl_3$): δ 1.23 (t, J = 6.0 Hz, 12H,), 3.69 (s, 8H), 4.15−4.20 (m, 12H), 5.15 (s, 2H), 6.65 (d, J = 8.8 Hz, 2H), 6.87 (d, J = 8.8 Hz, 2H), 7.62 (d, J = 8.0 Hz, 2H), 7.82 (t, J = 7.6 Hz, 2H), 8.47 (s, 2H), 8.50 (s, 2H). ^{13}C NMR (100 MHz, $CDCl_3$): δ 14.08, 55.01, 59.40, 60.70, 61.89, 116.19, 116.40, 118.89, 120.04, 120.95, 124.10, 138.89, 149.01, 154.56, 155.16, 159.85, 168.96, 172.85. ESI-MS (m/z): 757.3 ([M + H]$^+$, 100%), 779.2 ([M + Na]$^+$, 80%).

AMTTA. A mixture of compound **5** (230 mg, 0.31 mmol), KOH (0.45 g, 8.04 mmol), 1.13 mL of water, and 13 mL of ethanol was stirred at room temperature for 20 h. After evaporation, the residue was dissolved in 3 mL of water, and the pH of the solution was adjusted to ∼3 with HCl (3 M). The suspension was stirred for a further 20 h at room temperature, and then the precipitate was collected by filtration. After drying, the precipitate was added to 30 mL of dry acetonitrile, and the mixture was refluxed for 30 min. The precipitate was filtered and dried to afford AMTTA as a light-brown solid (122 mg, 61% yield). ^{1}H NMR (400 MHz, DMSO-d_6): δ 3.56 (s, 8H), 4.10 (s, 4H), 5.30 (s, 2H), 6.85 (d, J = 8.8 Hz, 2H), 6.98 (d, J = 8.8 Hz, 2H), 7.65 (d, J = 7.6 Hz, 2H), 7.99 (t, J = 7.6 Hz, 2H), 8.47 (s, 2H), 8.50 (d, J = 8.0 Hz, 2H). ^{13}C NMR (100 MHz, DMSO-d_6): δ 54.82, 59.72, 68.92, 116.21, 116.41, 118.95, 119.82, 120.45, 123.80, 138.44, 149.32, 154.07, 154.63, 155.55, 159.25, 172.85. Elem anal. Calcd for $C_{32}H_{32}N_6O_9\cdot 2.5H_2O$ (AMTTA·2.5H_2O): C, 55.73; H, 5.41; N, 12.19. Found: C, 55.50; H, 5.05; N, 11.94. ESI-MS (m/z): 643.2 ([M − H]$^-$, 100%), 321.1 ([M − 2H]$^{2-}$, 80%).

HTTA. A mixture of compound **3** (99 mg, 0.15 mmol), KOH (0.19 g, 3.39 mmol), 0.52 mL of water, and 6.3 mL of ethanol was stirred at room temperature for 20 h. After evaporation, the residue was dissolved in 2 mL of water, and the pH of the solution was adjusted to ∼3 with HCl (3 M). The suspension was stirred for a further 20 h at room temperature, and then the precipitate was collected by filtration. After drying, the precipitate was added to 30 mL of dry acetonitrile, and the mixture was refluxed for 30 min. The precipitate was filtered and dried to afford HTTA as a white solid (43 mg, 51% yield). ^{1}H NMR (400 MHz, DMSO-d_6): δ 3.63 (s, 8H), 4.16 (s, 4H), 4.73 (s, 2H), 7.65 (d, J = 7.6 Hz, 2H), 8.00 (t, J = 7.6 Hz, 2H), 8.40 (s, 2H), 8.51 (d, J = 8.0 Hz, 2H). ^{13}C NMR (100 MHz, DMSO-d_6): δ 54.80, 59.75, 62.42, 118.52, 119.86, 123.68, 138.44, 154.51, 154.91, 155.11, 158.92, 172.78. Elem anal. Calcd for $C_{26}H_{27}N_5O_9\cdot H_2O$ (HTTA·H_2O): C, 54.64; H, 5.11; N, 12.25. Found: C, 54.93; H, 4.86; N, 11.90. ESI-MS (m/z): 552.2 ([M − H]$^-$, 100%).

Syntheses of the Ln^{3+} Complexes. Stock solutions of AMTTA-Ln^{3+} and HTTA-Ln^{3+} (Ln = Eu and Tb) complexes were prepared by in situ mixing equivalent molar of the ligand (0.01 mmol) and $LnCl_3\cdot 6H_2O$ (0.01 mmol) in 5.0 mL of 50 mM HEPES buffer of pH 7.2. Stock solutions of the AMTTA-Eu^{3+}/Tb^{3+} and HTTA-Eu^{3+}/Tb^{3+} mixtures (ligand/Eu^{3+}/Tb^{3+} = 2/1/1) were prepared by adding the ligand (0.01 mmol), $TbCl_3\cdot 6H_2O$ (0.005 mmol), and $EuCl_3\cdot 6H_2O$ (0.005 mmol) into 5.0 mL of 50 mM HEPES buffer of pH 7.2. All stock solutions were stored at room temperature and suitably diluted with aqueous buffers before use. ESI-MS (m/z) for AMTTA-Eu^{3+}: 817.0 ([M + Na]$^+$, 100%), 795.1 ([M + H]$^+$, 70%). ESI-MS (m/z) for AMTTA-Tb^{3+}: 823.3 ([M + Na]$^+$, 100%), 801.2 ([M + H]$^+$, 70%). ESI-MS (m/z) for HTTA-Eu^{3+}: 724.6 ([M − 2H + Na]$^-$, 100%), 702.6 ([M − H]$^-$, 70%). ESI-MS (m/z) for HTTA-Tb^{3+}: 730.6 ([M − 2H + Na]$^-$, 100%), 708.6 ([M − H]$^-$, 70%).

Ratiometric Luminescence Detection of hROS in Aqueous Media. The reactions of the AMTTA-Eu^{3+}/Tb^{3+} mixture (total concentration of 20 μM; Eu^{3+}/Tb^{3+} = 1/1) with different concentrations of ClO^- and $^\bullet$OH were carried out in 50 mM HEPES buffer of pH 7.2. The ClO^- solutions with different concentrations were prepared by dilution of a stock solution of sodium hypochlorite and directly added into the AMTTA-Eu^{3+}/Tb^{3+} solution. As for $^\bullet$OH luminescence detection, different concentrations of $^\bullet$OH were in situ generated by adding Fe^{2+} (60 μM) and different concentrations of H_2O_2 into the AMTTA-Eu^{3+}/Tb^{3+} solution. All of the above reaction solutions were stirred at room temperature for 30 min and then subjected to time-gated luminescence measurement on a Perkin-Elmer LS 50B luminescence spectrometer.

Reactions of AMTTA-Ln^{3+} with Different ROS. The reactions of AMTTA-Ln^{3+} (10 μM AMTTA-Eu^{3+}, 10 μM AMTTA-Tb^{3+}, or a mixture of 10 μM AMTTA-Eu^{3+} and 10 μM AMTTA-Tb^{3+}) with ClO^- (15 μM NaClO), $^\bullet$OH (80 μM Fe^{2+} + 80 μM H_2O_2), NO (100 μM NOC-13), H_2O_2 (100 μM), NO_2^- (100 μM $NaNO_2$), $ONOO^-$ (100 μM NaONOO), and $O_2^{\cdot-}$ (100 μM xanthine + 100 μM xanthine oxidase) were carried out in 50 mM HEPES buffer of pH 7.2. The reaction with $^1O_2$ (1.0 mM Na_2MoO_4 + 100 μM H_2O_2) was carried out in 50 mM carbonate buffer of pH 10.5. All of the solutions were stirred at room temperature for 30 min and then subjected to time-gated luminescence measurement on a Perkin-Elmer LS 50B luminescence spectrometer.

RESULTS AND DISCUSSION

Design and Photophysical Properties of the Ln^{3+} Complexes. To design a ratiometric fluorescence probe, it is vital that two emissions of the probe at different wavelengths should originate from the same excited state, allowing the emission intensity ratio to be independent of the concentration, photobleaching, and power fluctuation of the excitation source. Recently, a robust approach using a heterometallic bis(lanthanide) ensemble for the design of ratiometric luminescence probes has been reported, wherein a mixture of Eu^{3+} and Tb^{3+} complexes outfitted with the same antenna ligand to display both the Eu^{3+} and Tb^{3+} emissions having different responses to the analyte could be combined.[28] In this work, we designed and synthesized a novel dual-functional ligand, AMTTA, by incorporating an electron-rich group, *p*-aminophenyl, into a strongly coordinating antenna, (2,2′:6′,2″-terpyridine-6,6″-diyl)bis(methylenenitrilo)tetrakis(acetic acid), capable of sensitizing the luminescence of both Eu^{3+} and Tb^{3+} ions.[29] The *p*-aminophenyl group in the AMTTA-Ln^{3+} complex has two functions. One is to quench the Ln^{3+} luminescence via a PET process to make the Ln^{3+} luminescence be turned-off,

dx.doi.org/10.1021/ic202195a | Inorg. Chem. 2012, 51, 2940−2946

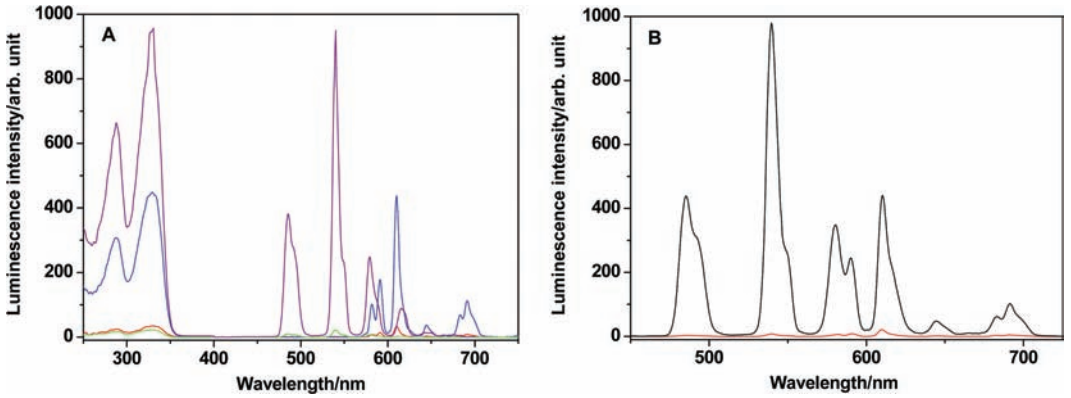

Figure 1. (A) Time-gated excitation and emission spectra of AMTTA-Ln^{3+} (3.5 μM, red line for AMTTA-Eu^{3+}, green line for AMTTA-Tb^{3+}) and HTTA-Ln^{3+} (3.5 μM, blue line for HTTA-Eu^{3+}, purple line for HTTA-Tb^{3+}) in 50 mM borate buffer of pH 9.1. (B) Emission spectra of the AMTTA-Eu^{3+}/Tb^{3+} mixture (total concentration of 7.0 μM; Eu^{3+}/Tb^{3+} = 1/1; red line) and HTTA-Eu^{3+}/Tb^{3+} mixture (total concentration of 7.0 μM; Eu^{3+}/Tb^{3+} = 1/1; black line) in 50 mM borate buffer of pH 9.1.

and the other is to enable the complex to selectively react with hROS to cleave the *p*-aminophenyl ether from the ligand. Thus, the weakly luminescent AMTTA-Eu^{3+}/Tb^{3+} mixture is expected to serve as a ratiometric luminescence probe for hROS because the mixture could be considered to display different responses at Eu^{3+} and Tb^{3+} emissions toward hROS based on the different emission efficiencies of the cleavage reaction products, HTTA-Eu^{3+} and HTTA-Tb^{3+}.[29]

The photophysical properties of AMTTA-Eu^{3+}, AMTTA-Tb^{3+}, HTTA-Eu^{3+}, and HTTA-Tb^{3+} were measured in 50 mM borate buffer of pH 9.1. As shown in Figure 1A, the two AMTTA-Ln^{3+} complexes are weakly luminescent with very low quantum yields ($\varepsilon_{331\ nm}$ = 1.37 × 10^4 cm^{-1} M^{-1}, ϕ = 0.59%, and τ = 1.02 ms for AMTTA-Eu^{3+}; $\varepsilon_{331\ nm}$ = 1.35 × 10^4 cm^{-1} M^{-1}, ϕ = 0.19%, and τ = 0.39 ms for AMTTA-Tb^{3+}). However, after reacting with hROS to afford HTTA-Ln^{3+}, the complexes become highly luminescent with remarkable increases of their quantum yields and luminescence lifetimes ($\varepsilon_{331\ nm}$ = 1.36 × 10^4 cm^{-1} M^{-1}, ϕ = 16.3%, and τ = 1.38 ms for HTTA-Eu^{3+}; $\varepsilon_{331\ nm}$ = 1.38 × 10^4 cm^{-1} M^{-1}, ϕ = 11.5%, and τ = 1.22 ms for HTTA-Tb^{3+}). The product of AMTTA-Tb^{3+} reacting with ClO^- was confirmed by time-of-flight ESI-MS spectrum (Figure S1 in the Supporting Information), in which the base peak at *m*/*z* 708.0745 could be assigned to be the molecular ion peak of HTTA-Tb^{3+}. All of the Ln^{3+} complexes are highly stable in aqueous media because of the nonadentate terpyridine–polyacid structure of the ligand.[18c,27]

The time-gated emission spectra of mixtures of AMTTA-Eu^{3+}/Tb^{3+} and HTTA-Eu^{3+}/Tb^{3+} (ligand/Eu^{3+}/Tb^{3+} = 2/1/1) in 50 mM borate buffer of pH 9.1 are shown in Figure 1B. Because both of the Eu^{3+} and Tb^{3+} complexes were outfitted with the same antenna chromophore, the "cocktails" of the complexes showed simultaneously Eu^{3+} emission at 610 nm ($^5D_0 \rightarrow {}^7F_2$) and Tb^{3+} emission at 540 nm ($^5D_4 \rightarrow {}^7F_5$) when excited at the same wavelength (maximum at 331 nm). In fact, when the AMTTA-Eu^{3+}/Tb^{3+} mixture was reacted with hROS, the emission color of the weakly luminescent solution turned strongly yellow (Scheme 1), the mixed color of green emission from HTTA-Tb^{3+} and red emission from HTTA-Eu^{3+}. In addition, Figure 1B also shows that the intensity of Eu^{3+} emission (610 nm) is ~5-fold higher than that of Tb^{3+} emission (540 nm) in the spectrum of the AMTTA-Eu^{3+}/Tb^{3+} mixture, while the intensity of Eu^{3+} emission (610 nm) is only half that of Tb^{3+} emission (540 nm) in the spectrum of the HTTA-Eu^{3+}/Tb^{3+} mixture. These results indicate that the luminescence response sensitivity of AMTTA-Tb^{3+} at 540 nm is remarkably higher than that of AMTTA-Eu^{3+} at 610 nm toward hROS, suggesting that the AMTTA-Eu^{3+}/Tb^{3+} mixture could be used as a ratiometric probe for the time-gated luminescence detection of hROS with the I_{540}/I_{610} ratio as a signal.

Time-Gated Luminescence Detection of hROS Using AMTTA-Eu^{3+}/Tb^{3+} as a Ratiometric Probe. Quantitative time-gated luminescence detections of $^{\bullet}OH$ and ClO^- using the AMTTA-Eu^{3+}/Tb^{3+} mixture (10 μM AMTTA-Eu^{3+} + 10 μM AMTTA-Tb^{3+}) as a ratiometric probe were carried out in 50 mM HEPES buffer of pH 7.2. Because $^{\bullet}OH$ was in situ generated by the Fenton reaction, before $^{\bullet}OH$ detection, it was confirmed that the probe could not react with H_2O_2 or Fe^{2+} by reacting the AMTTA-Eu^{3+}/Tb^{3+} mixture with H_2O_2 or Fe^{2+} alone (no time-gated luminescence response was observed). However, in the presence of Fe^{2+}, the intensities of both Eu^{3+} and Tb^{3+} emissions of the probe were significantly increased upon the addition of H_2O_2. These results clearly indicate that the luminescence enhancement of the probe was caused by $^{\bullet}OH$ and not by H_2O_2 or Fe^{2+} species.

Figure 2 shows the time-gated emission spectra of the probe in the presence of Fe^{2+} (60 μM) and different concentrations of H_2O_2 in the buffer. Although the intensities of the probe at Eu^{3+} and Tb^{3+} emissions were simultaneously increased because of the different luminescence response behaviors of AMTTA-Eu^{3+} and AMTTA-Tb^{3+} to $^{\bullet}OH$, the reaction between the probe and $^{\bullet}OH$ gave rise to an increase of the I_{540}/I_{610} ratio from 0.18 to 1.4 to provide a comfortable 7.8-fold contrast window in which to detect $^{\bullet}OH$ radicals. The inset curve in Figure 2, fitted to a double-exponential correlation, shows the variation of the I_{540}/I_{610} ratio as a function of the H_2O_2 concentration, in which a good linear correlation between the I_{540}/I_{610} ratio and H_2O_2 concentration (Figure S2 in the Supporting Information) can be fitted in the lower concentration range of H_2O_2 (5.0–30 μM, which can be considered to correspond to the concentration range of $^{\bullet}OH$ because one H_2O_2 molecule can generate one $^{\bullet}OH$ in the presence of excess Fe^{2+}).[30] This result demonstrated the feasibility of the ratiometric probe for the quantitative time-gated luminescence detection of $^{\bullet}OH$ radicals.

Figure 3 shows the time-gated emission spectra of the probe in the presence of different concentrations of ClO^- in the

dx.doi.org/10.1021/ic202195a | *Inorg. Chem.* 2012, 51, 2940–2946

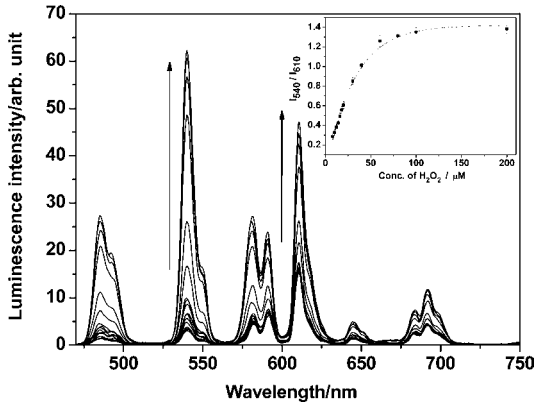

Figure 2. Time-gated emission spectra (λ_{ex} = 331 nm) of the AMTTA-Eu^{3+}/Tb^{3+} mixture (total concentration of 20 μM, Tb^{3+}/Eu^{3+} = 1/1) in the presence of Fe^{2+} (60 μM) and different concentrations of H_2O_2 (0.0, 2.0, 4.0, 6.0, 8.0, 10, 12, 14, 16, 18, 20, 30, 40, 60, 80, 100, and 200 μM) in 50 mM HEPES buffer of pH 7.2. The inset shows the intensity ratio of I_{540}/I_{610} as a function of the H_2O_2 concentration.

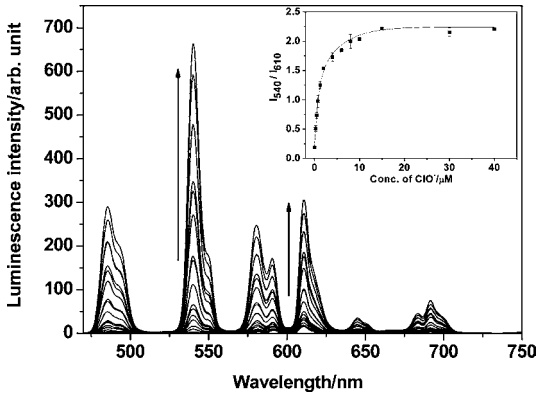

Figure 3. Time-gated emission spectra (λ_{ex} = 331 nm) of the AMTTA-Eu^{3+}/Tb^{3+} mixture (total concentration of 20 μM; Eu^{3+}/Tb^{3+} = 1/1) in the presence of different concentrations of ClO^- (0.0, 0.25, 0.5, 0.75, 1.0, 1.25, 1.5, 2.0, 3.0, 4.0, 6.0, 8.0, 10, 15, 20, 30, and 40 μM) in 50 mM HEPES buffer of pH 7.2. The inset shows the intensity ratio of I_{540}/I_{610} as a function of the ClO^- concentration.

buffer. Compared to the response to $^{\bullet}OH$, the probe showed a higher sensitivity to respond to ClO^- with a faster increase of its I_{540}/I_{610} ratio at low concentrations of ClO^- (the I_{540}/I_{610} ratio reached to the maximum value upon the addition of 10 μM ClO^-), and the variation of the I_{540}/I_{610} ratio against the ClO^- concentration (the inset in Figure 3), fitted also to a double-exponential correlation, provided a broader contrast window from 0.18 to 2.23 (12.3-fold) for the detection of ClO^-. We also investigated the luminescent responses of AMTTA-Eu^{3+} (10 μM) and AMTTA-Tb^{3+} (10 μM) toward ClO^-, respectively. As shown in Figure S3B in the Supporting Information, after reaction with ClO^-, the ratio of the Tb^{3+} and Eu^{3+} emissions (I_{540}/I_{610}) increased from 0.19 to 2.16 (11.4-fold), which is almost the same as that of the AMTTA-Eu^{3+}/Tb^{3+} mixture and indicates that the effect of the differential metal displacement of the lanthanide complexes caused by hROS on the ratiometric detection is small and can be negligible. To examine the response kinetics of the probe toward ClO^-, the real-time luminescence responses of AMTTA-Tb^{3+} (10 μM) to the repeat additions of ClO^- (3.0 μM) in 50 mM HEPES buffer of pH 7.2 were determined. As shown in Figure 4, the luminescence intensity of AMTTA-Tb^{3+} itself was very weak and stable but could be increased

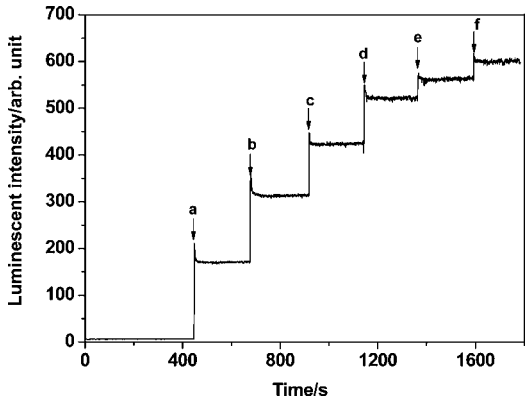

Figure 4. Time course of the luminescence response of AMTTA-Tb^{3+} (10 μM) to the addition of ClO^- in 50 mM HEPES buffer of pH 7.2 at room temperature (the 3.0 μM ClO^- solution was added six times at a, b, c, d, e, and f, respectively). The luminescence intensity at 540 nm was determined (λ_{ex} = 331 nm).

immediately to reach the maximum value and then kept at a steady level for a long time upon the addition of ClO^-. This result indicates that the reaction between AMTTA-Ln^{3+} and ClO^- is very fast, which is favorable for the detection of ClO^- in complicated samples to avoid the effects of other undesirable reactions.

Effects of the pH and ROS. The effects of the pH on the I_{540}/I_{610} ratios of the AMTTA-Eu^{3+}/Tb^{3+} (5.0 μM AMTTA-Eu^{3+} + 5.0 μM AMTTA-Tb^{3+}) and HTTA-Eu^{3+}/Tb^{3+} (5.0 μM HTTA-Eu^{3+} + 5.0 μM HTTA-Tb^{3+}) mixtures were investigated in 50 mM Tris-HCl buffers with different pHs ranging from 4 to 10. As shown in Figure 5, the I_{540}/I_{610} ratios of the AMTTA-

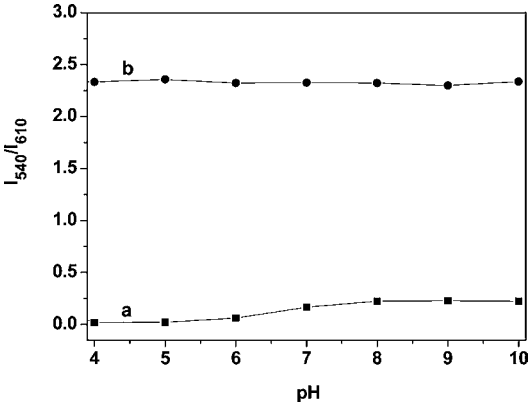

Figure 5. Effects of the pH on the I_{540}/I_{610} ratios of AMTTA-Eu^{3+}/Tb^{3+} (a, total concentration of 10 μM, Eu^{3+}/Tb^{3+} = 1/1) and HTTA-Eu^{3+}/Tb^{3+} (b, total concentration of 10 μM, Eu^{3+}/Tb^{3+} = 1/1) in 50 mM Tris-HCl buffers with different pHs.

Eu^{3+}/Tb^{3+} and HTTA-Eu^{3+}/Tb^{3+} mixtures are not remarkably affected by the pH value, which suggests that the AMTTA-Eu^{3+}/Tb^{3+} mixture could work well as a ratiometric probe for the time-gated luminescence detection of hROS in weakly acidic, neutral, and weakly basic buffers.

To evaluate the response specificity of the probe to hROS, the reactions of AMTTA-Eu^{3+} (10 μM), AMTTA-Tb^{3+} (10 μM), and the AMTTA-Eu^{3+}/Tb^{3+} mixture (10 μM AMTTA-

dx.doi.org/10.1021/ic202195a | Inorg. Chem. 2012, 51, 2940–2946

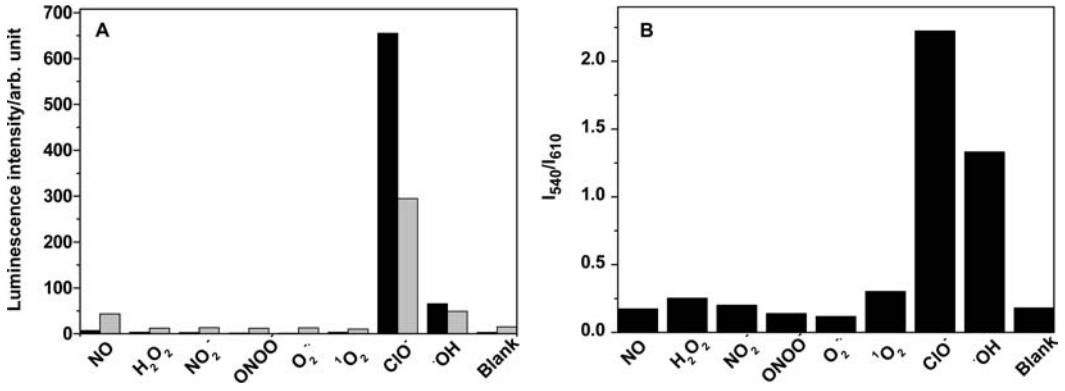

Figure 6. (A) Luminescence intensities of the products of AMTTA-Tb^{3+} (10 μM, black column) and AMTTA-Eu^{3+} (10 μM, gray column) reacted with various ROS in 50 mM HEPES buffer of pH 7.2. (B) I_{540}/I_{610} ratios of the products of the AMTTA-Eu^{3+}/Tb^{3+} mixture (total concentration of 20 μM, Tb^{3+}/Eu^{3+} = 1/1) reacted with various ROS in 50 mM HEPES buffer of pH 7.2.

Eu^{3+} + 10 μM AMTTA-Tb^{3+}) with various ROS were carried out in 50 mM HEPES buffer of pH 7.2. As shown in Figure 6A, both AMTTA-Eu^{3+} and AMTTA-Tb^{3+} almost did not give observable luminescence responses to the addition of excess (100 μM) NO, H_2O_2, NO_2^-, $ONOO^-$, $O_2^{\bullet-}$, and $^1O_2$, whereas the luminescence intensities of AMTTA-Tb^{3+} and AMTTA-Eu^{3+} were 233- and 19-fold increased upon the addition of ClO^- (15 μM) and 23- and 3.2-fold increased upon the addition of $^{\bullet}OH$ (80 μM). These results indicate that AMTTA-Ln^{3+} cannot react with other ROS apart from $^{\bullet}OH$ and ClO^-, so that the AMTTA-Eu^{3+}/Tb^{3+} mixture can be used as a ratiometric probe for hROS with high specificity. Indeed, when the AMTTA-Eu^{3+}/Tb^{3+} mixture was reacted with various ROS, the I_{540}/I_{610} ratio of the mixture did not show remarkable responses to NO, H_2O_2, NO_2^-, $ONOO^-$, $O_2^{\bullet-}$, and $^1O_2$ (the change <0.1), while that was 7.8- and 12.3-fold increased after reaction with $^{\bullet}OH$ and ClO^-, respectively (Figure 6B).

CONCLUSION

In this work, by incorporating an aminophenyl group into (2,2′:6′,2″-terpyridine-6,6″-diyl)bis(methylenenitrilo)tetrakis-(acetic acid), a dual-functional ligand, AMTTA, that can form highly stable complexes with Eu^{3+} and Tb^{3+} ions and specifically react with hROS in aqueous media was designed and synthesized. Upon reaction with hROS, the weakly luminescent "cocktail" of AMTTA-Eu^{3+} and AMTTA-Tb^{3+} can exhibit a highly structured, strong, and information-rich composite luminescence spectrum under a single-wavelength excitation with a remarkable increase of its I_{540}/I_{610} ratio, which provides a useful ratiometric probe for the time-gated luminescence detection of hROS. Compared to the reported hROS fluorescence probes, the new probe has the advantages of high water solubility and stability, wide pH available range, and applicability for ratiometric and time-gated luminescence detection, which would be a useful tool for investigating the pathogenic role of hROS in complicated biological systems. Though AMTTA-Ln^{3+} is not cell-membrane-permeable because of its electronegative ([AMTTA-Ln]$^-$) property, appropriate modification of its structure is ongoing for cellular use.

ASSOCIATED CONTENT

Supporting Information

Schematic pathways for the synthesis of AMTTA and HTTA and three supplementary figures. This material is available free of charge via the Internet at http://pubs.acs.org.

AUTHOR INFORMATION

Corresponding Author

*E-mail: zhiqiangye2001@yahoo.com.cn (Z.Y.), jingliyuan@yahoo.com.cn (J.Y.). Phone/Fax: +86-411-84986041.

Notes

The authors declare no competing financial interest.

ACKNOWLEDGMENTS

Financial support from the National Natural Science Foundation of China (Grant 20835001) is gratefully acknowledged.

REFERENCES

(1) D'Autréaux, B.; Toledano, M. B. *Nat. Rev. Mol. Cell. Biol.* **2007**, *8*, 813−824.
(2) Valko, M.; Leibfritz, D.; Moncol, J.; Cronin, M. T. D.; Mazur, M.; Telser, J. *Int. J. Biochem. Cell Biol.* **2007**, *39*, 44−84.
(3) Winterbourn, C. C. *Nat. Chem. Biol.* **2008**, *4*, 278−286.
(4) Wiseman, H.; Halliwell, B. *Biochem. J.* **1996**, *313*, 17−29.
(5) McCord, J. M. *Science* **1974**, *185*, 529−531.
(6) Dobashi, K.; Ghosh, B.; Orak, J. K.; Singh, I.; Singh, A. K. *Mol. Cell. Biochem.* **2000**, *205*, 1−11.
(7) Nishida, M.; Maruyama, Y.; Tanaka, R.; Kontani, K.; Nagao, T.; Kurose, H. *Nature* **2000**, *408*, 492−495.
(8) Frohlich, K. U.; Madeo, F. *FEBS Lett.* **2000**, *473*, 6−9.
(9) Schmidt, K. N.; Amstad, P.; Cerutti, P.; Baeuerle, P. A. *Chem. Biol.* **1995**, *2*, 13−22.
(10) Yermolaieva, O.; Brot, N.; Weissbach, H.; Heinemann, S. H.; Hoshi, T. *Proc. Natl. Acad. Sci. U.S.A.* **2000**, *97*, 448−453.
(11) (a) Dickinson, B. C.; Chang, C. J. *Nat. Chem. Biol.* **2011**, *7*, 504−511. (b) Yasui, H.; Sakurai, H. *Biochem. Biophys. Res. Commun.* **2000**, *269*, 131−136. (c) Kuppusamy, P.; Chzhan, M. V. K.; Shteynbuk, M.; Lefer, D. J.; Giannella, E.; Zweier, J. L. *Proc. Natl. Acad. Sci. U.S.A.* **1994**, *91*, 3388−3392.
(12) (a) Grynkiewicz, G.; Poenie, M.; Tsien, R. Y. *J. Biol. Chem.* **1985**, *260*, 3440−3450. (b) Minta, A.; Kao, J. P. Y.; Tsien, R. Y. *J. Biol. Chem.* **1989**, *264*, 8171−8178.
(13) (a) Hempel, S. L.; Buettner, G. R.; O'Malley, Y. Q.; Wessels, D. A.; Flaherty, D. M. *Free Radical Biol. Med.* **1999**, *27*, 146−159. (b) Kooy, N. W.; Royall, J. A.; Ischiropoulos, H.; Beckman, J. S. *Free Radical Biol. Med.* **1994**, *16*, 149−156.

(14) (a) Dickinson, B. C.; Peltier, J.; Stone, D.; Schaffer, D. V.; Chang, C. J. *Nat. Chem. Biol.* **2011**, *7*, 106−112. (b) Miller, E. W.; Tulyanthan, O.; Isacoff, E. Y.; Chang, C. J. *Nat. Chem. Biol.* **2007**, *3*, 263−267.
(15) Setsukinai, K.; Urano, Y.; Kakinuma, K.; Majima, H. J.; Nagano, T. *J. Biol. Chem.* **2003**, *278*, 3170−3175.
(16) Koide, Y.; Urano, Y.; Kenmoku, S.; Kojima, H.; Nagano, T. *J. Am. Chem. Soc.* **2007**, *129*, 10324−10325.
(17) (a) Srikun, D.; Miller, E. W.; Domaille, D. W.; Chang, C. J. *J. Am. Chem. Soc.* **2008**, *130*, 4596−4597. (b) Lin, W.; Long, L.; Chen, B.; Tan, W. *Chem.—Eur. J.* **2009**, *15*, 2305−2309. (c) Kiyose, K.; Kojima, H.; Urano, Y.; Nagano, T. *J. Am. Chem. Soc.* **2006**, *128*, 6548−6549. (d) Zhang, X. L.; Xiao, Y.; Qian, X. H. *Angew. Chem., Int. Ed.* **2008**, *47*, 8025−8029.
(18) (a) Poole, R. A.; Kielar, F.; Richardson, S. L.; Stenson, P. A.; Parker, D. *Chem. Commun.* **2006**, 4084−4086. (b) Law, G. L.; Pal, R.; Palsson, L. O.; Parker, D.; Wong, K. L. *Chem. Commun.* **2009**, 7321−7323. (c) Song, C. H.; Ye, Z. Q.; Wang, G. L.; Yuan, J. L.; Guan, Y. F. *Chem.—Eur. J.* **2010**, *16*, 6464−6472. (d) Lewis, D. J.; Glover, P. B.; Solomons, M. C.; Pikramenou, Z. *J. Am. Chem. Soc.* **2011**, *133*, 1033−1043.
(19) (a) Galaup, C.; Couchet, J. M.; Bedel, S.; Tisnès, P.; Picard, C. *J. Org. Chem.* **2005**, *70*, 2274−2284. (b) Petitjean, A.; Kyritsakas, N.; Lehn, J. M. *Chem.—Eur. J.* **2005**, *11*, 6818−6828.
(20) Hrabie, J. A.; Klose, J. R.; Wink, D. A.; Keefer, L. K. *J. Org. Chem.* **1993**, *58*, 1472−1476.
(21) Lei, B.; Adachi, N.; Arai, T. *Brain Res. Protoc.* **1998**, *3*, 33−36.
(22) Charkoudian, L. K.; Pham, D. M.; Franz, K. J. *J. Am. Chem. Soc.* **2006**, *128*, 12424−12425.
(23) Reed, J. W.; Ho, H. H.; Jolly, W. L. *J. Am. Chem. Soc.* **1974**, *96*, 1248−1249.
(24) Yang, D.; Wang, H. L.; Sun, Z. N.; Chung, N. W.; Shen, J. G. *J. Am. Chem. Soc.* **2006**, *128*, 6004−6005.
(25) Aubry, J. M.; Cazin, B. *Inorg. Chem.* **1988**, *27*, 2013−2014.
(26) Xu, K. H.; Liu, X.; Tang, B.; Yang, G. W.; Yang, Y.; An, L. G. *Chem.—Eur. J.* **2007**, *13*, 1411−1416.
(27) Song, B.; Wang, G. L.; Tan, M. Q.; Yuan, J. L. *J. Am. Chem. Soc.* **2006**, *128*, 13442−13450.
(28) Tremblay, M. S.; Halim, M.; Sames, D. *J. Am. Chem. Soc.* **2007**, *129*, 7570−7577.
(29) Latva, M.; Takalo, H.; Mukkala, V. M.; Matachescu, C.; Rodríguez-Ubis, J. C.; Kankare, J. *J. Lumin.* **1997**, *75*, 149−169.
(30) Luehrs, D. C.; Roher, A. E.; Wright, S. W. *J. Chem. Educ.* **2007**, *84*, 1290−1291.